Micromachined silicon Generator for Harvesting Power from Vibrations

S. P. Beeby, M. J. Tudor, E. Koukharenko, N. M. White, T. O'Donnell*, C. Saha*, S. Kulkarni*, S. Roy*

University of Southampton, School of Electronics and Computer Science, Southampton SO17 1BJ, UK.

*NMRC, Prospect Row, Cork, Ireland.

Abstract

This paper describes the design, simulation and fabrication of an electromagnetic device for generating electrical energy from vibrations. A range of dimensions has been simulated using ANSYS in order to determine natural frequencies and material stresses. A 300μm wide paddle beam gives a natural frequency of 6.4 kHz for the mode of operation and induced stresses at maximum amplitudes are well within material limits. Ansoft's Maxwell 2D has been used to predict the voltages generated and an integrated electroplated coil of 71 turns produces 0.38V with no load. Devices are currently being fabricated and the process is described.

Keywords: Kinetic energy harvesting, energy from vibrations, electromagnetic generator, simulation

1 INTRODUCTION

The rapid growth in the field of wireless sensor networks has highlighted the issue of powering remote sensor nodes. The requirement to change batteries, or refuel other power sources, places an unwanted additional maintenance and cost burden on such wireless networks. In certain applications where environmental vibrations are present, there is the opportunity to harvest the kinetic energy of these vibrations and use this to power the remote sensor node [i].

This paper introduces the design of an electromagnetic micromachined silicon generator. The results from comprehensive simulation of both the mechanical and magnetic characteristics of the device, and the optimum design, are presented. Finally, the silicon micromachining approach currently being employed to fabricate the devices is discussed.

2 ELECTROMAGNETIC MICROMACHINED SILICON GENERATOR DESIGN

The micromachined generator is based upon a larger design developed at the University of Southampton using metal components and conventional machining processes [ii]. This generator uses a four magnet configuration, with the magnets located on a stainless steel beam designed to vibrate at resonance. The resonant frequency is adjustable about a nominal value of 100Hz. A coil is located between the 4 magnets such that the flux lines and the direction of motion are perpendicular to the coil windings. The configuration is shown in figure 1. This design has been fully characterised and presents a highly efficient configuration [iii].
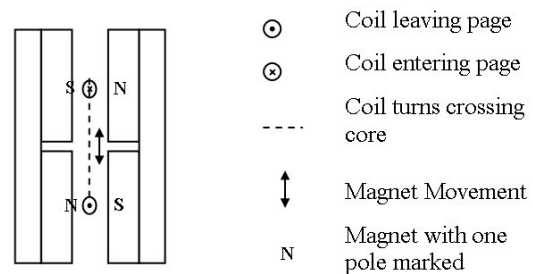

Fig. 1 Original generator configuration.

The micro generator, shown in figure 2, is therefore based upon this configuration and is designed to be realisable using standard silicon micromachining techniques. Figure 2 shows a four magnet arrangement in which the coil is designed to move laterally relative to the magnets.
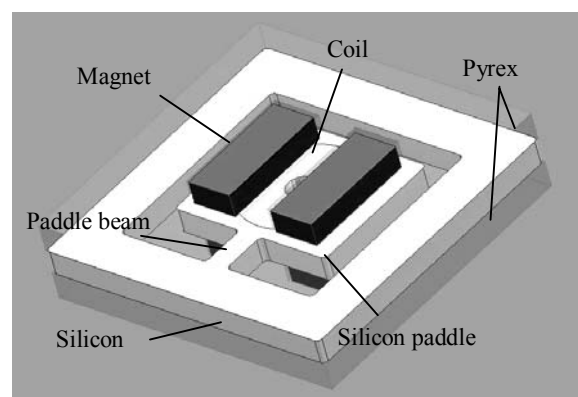

Fig. 2 Micromachined silicon generator

Two magnets are located within etched recesses in the Pyrex wafers and two Pyrex wafers are anodically bonded to each face of the silicon wafer. The coil is located on a silicon cantilevered paddle designed to vibrate laterally in the plane of the wafer. The bonding process is aligned to ensure

correct placement of the coil relative to the magnets and the paddle will be deep reactive ion etched (DRIE) through the thickness of the wafer. Electrical connection is provided by bond pads located at the die perimeter.

3 MECHANICAL MODELLING

The mechanical characteristics of the dynamic component of the generator (the cantilevered silicon paddle) have been simulated using ANSYS finite element analysis (FEA). A modal analysis is used to determine the resonant frequencies of different cantilever configurations. Mechanical stresses induced by the deformation have also been simulated in order to ensure the structure can withstand repeated cyclical stressing at maximum amplitudes.

The generator has been simulated using a solid modelling technique. A series of keypoints is used to define the geometry of the device after which the ANSYS software automatically meshed the structure. Material properties are defined and boundary conditions applied, after which the particular analysis is performed. Three sets of supporting paddle beam dimensions have been simulated, each 1mm long and 0.5mm thick. Model A is 500μm wide, B 400μm wide and C 300μm wide. Table 1 lists the resonant frequencies of the first three modes of the different models simulated. Mode 1, shown viewed from above in figure 3, is the fundamental lateral vibration and the desired mode of operation of the generator. Mode 2 is the fundamental torsional mode and mode 3 is the fundamental out of plane resonance.

The amplitude of vibration is limited by the surrounding silicon frame which limits the displacement to 0.5mm. The device frame forms a physical over-range protection by limiting the motion of the paddle. This should protect the generator against excessive vibrations and shock loads. To evaluate the over-range protection a basic FEA stress analysis was performed at this maximum displacement. This simulation calculates the maximum stress level occurring at the maximum displacement for each model type and enables comparison with the yield stress of silicon. The results for each model are listed in column 4 of table 1. The yield stress of silicon is 7GPa and the values calculated are well below this limit.

Table 1 Modal frequencies

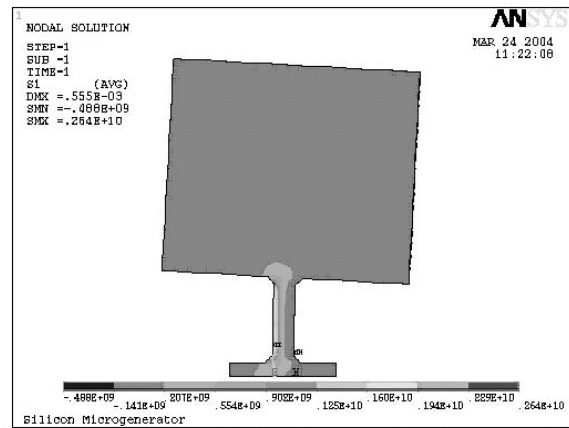| Model	Mode 1 (kHz)	Mode 2 (kHz)	Mode 3 (kHz)	Max stress
A	12.6	13.45	29.5	4.5
B	9.5	12.4	25.9	3.5
C	6.4	11	20	2.6

Fig. 3 Generator mode of operation

Paddle beam C is the most promising geometry since the smaller width reduces the resonant frequency of the structure compared to beams A and B. The reduced stiffness of this beam means that the structure is more flexible and the level of stress experienced at the maximum deflection is 2.6GPa. This is 4.4GPa below the yield strength of silicon and provided no defects are introduced during the fabrication, the single crystal nature of silicon and the fact it is elastic to fracture means the beam will withstand the maximum possible deflections without fracturing. The ultimate robustness of the generator will in practice be limited by surface and/or material imperfections and the impact stresses arising from the paddle contacting the frame. The stress analysis of the over-range protection presented here does not include these impact stresses.

4 MAGNETIC MODELLING

Electromagnetic FEA simulations using Ansoft's Maxwell 2D have also been performed to determine the voltages which can be generated from the above structure. The modelling has been performed on a micro-generator employing an integrated coil formed on the paddle using electroplated copper. As described later, a device with a traditional wound coil will also be fabricated and evaluated. The coil consists of a square spiral coil of 71 turns with each turn being 10 μm wide, 10 μm thick with a spacing between the turns of 10 μm. The calculated resistance of this coil is 77 Ohms. The magnets used are 1 mm x 1mm x 0.75 mm thick, sintered, NdFeB magnets. The results from an FEA simulation showing the flux density distribution from the magnets is shown in fig.4. As can be seen from the plot a flux density of approximately 0.5 T exists in the gap between the magnets.
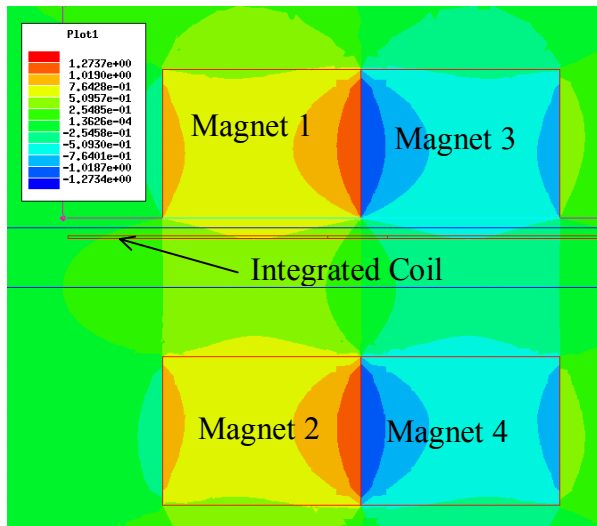
Figure 4 - Flux density plot for the micro-generator

In order to predict the voltage which will be generated by the micro-generator, 2D FEA simulations are performed using a transient simulation with a sinusoidal velocity input. The amplitude of the velocity is calculated so as to give the maximum displacement at the resonant frequency of the device as given in table 1. The maximum displacement is taken as the maximum displacement of the centre point of the paddle, when the corner point of the paddle is displaced (by a rotational motion) by 0.5 mm. This maximum displacement is calculated to be 0.14 mm. Table 2 gives the results for the voltages generated according to the FE simulation for all three beam geometries. The results are for the mode 1 vibration only. For the purposes of the 2D simulation the depth of model is assumed to be the mean diameter of the coil, which is 1.6 mm in this case.

Table 2: Finite element results for voltages generated

Model	Resonant frequency (kHz)	No load Voltage (V)
A	12.6	0.76
B	9.5	0.57
C	6.4	0.38

It can be seen that the higher the resonant frequency, the greater the generated voltage. For a fixed displacement, the higher frequency generator will have greater velocity and hence the voltage is increased. Because the simulation performed here is a 2D simulation, the motion of the paddle is a 2D translational motion. However in practice the paddle motion is a rotational motion, constrained by the bending of the beam. 3D simulation is required to more accurately model the paddle motion and this will be performed in the future.

5 FABRICATION

Initially two types of generator are being fabricated. The first will utilise discrete coils traditionally wound from enamelled copper wire. The coil has an internal diameter of 0.5mm, an external diameter of 2.4mm and a thickness of 0.5mm. The coil is being wound from 25μm diameter enamelled wire. Assuming a fill factor of 0.8, which is consistent with previous coils from the supplier, this equates to approximately 390 turns, a coil resistance of 109 Ohms and inductance of 210 μH. The coil will be positioned at the centre of the paddle and will locate within a hole etched through the silicon thickness. The second type will of generator will use integrated coils fabricated in paddle surface. The coil will be a two layer copper structure and will have up to 77 turns. The integrated coil is formed by electroplating and photolithography, as described below. The discrete coil approach offers a greater number of turns than can be achieved using integrated coils and should therefore yield higher voltages. The integrated coil approach offers full batch fabrication of the generator, but at the expense of fewer turns. Both types of generator are being fabricated to enable evaluation of their characteristics and experimental comparison between devices.

The fabrication process of the discrete coil generator is shown in figure 5. This process consists of first wet etching a trench for the coil wires to follow so that they lie below the surface of the wafer and do not prevent wafer bonding. Next aluminium is evaporated to a thickness of 1mm and patterned to define bond pads and tracks where required. Finally, the paddle and frame formed by DRIE etching through the thickness of the silicon wafer. The discrete coils will be manually positioned and connected to the bond pads.
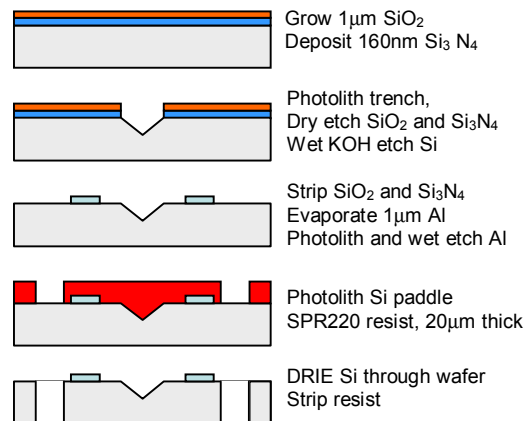

Figure 5 – Discrete coil generator fabrication

The fabrication of the integrated coil is shown in figure 6. The first coil layer is a 1μm thick Ti/Cu film sputtered on to a 4μm thick CVD SiO$_2$ layer. This is patterned and a second 4μm thick CVD SiO2 layer is deposited to insulate the coil layers. A window is opened in the insulating SiO$_2$ film and a 0.02/0.2μm Ti/Cu seed layer is sputtered across the wafers. Next, a 12μm thick layer of AZ 9260 resist is spun onto the wafer and the top coil layer defined by photolithography. The coil is then formed by

electroplating the wafers forming 10μm thick Cu tracks within the resist. The resist is then stripped and the seed layers etched by a dip etch in $CUSO_4+NH_4OH$ and HF for the Cu and Ti respectively.

CVD 4μm SiO_2
Sputter 1um Ti/Cu film

Photolith bottom coil layer
Etch Cu in Ammonium
Persulfate and Ti in HF

CVD 4μm SiO_2 and photolith contact via.
Wet etch SiO_2 and strip resist

Sputter Ti/Cu Seed layer
Spin 12mm thick resist and pattern top coil layer

Electroplate 10μm thick Cu layer
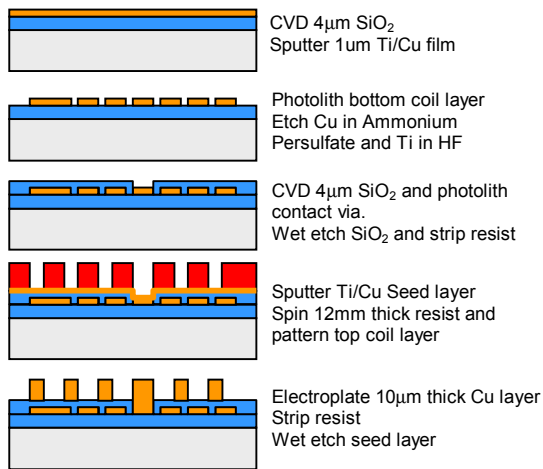Strip resist
Wet etch seed layer

Figure 6 – Integrated coil fabrication

The magnets are located in Pyrex wafers which are subsequently anodically bonded to the top and bottom faces of the wafer. The Pyrex wafers contain etched regions to form a cavity around the paddle in order to enable it to move. The area over the bond pads is also etched to allow subsequent access. A plan view and cross-section of the generator are shown in figures 7 and 8 respectively.
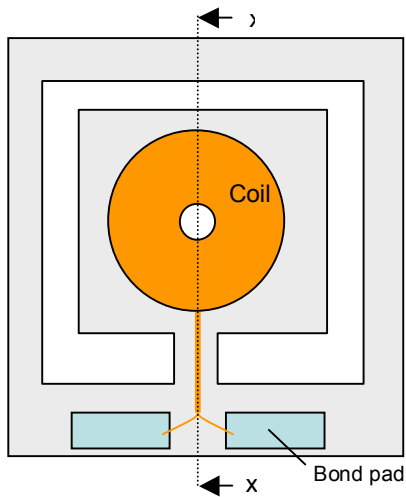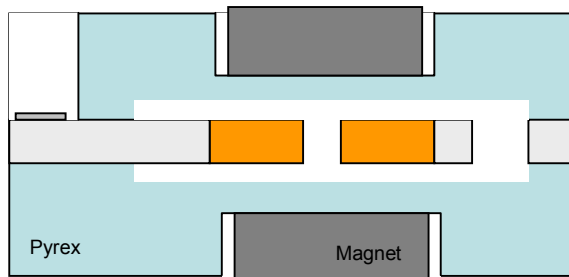

Figure 7 – plan view of generator

Figure 8 – cross section through x-x.

6 CONCLUSIONS

This paper presents the results from a comprehensive design study into the mechanical and electromagnetic behaviour of a silicon vibration powered generator. Of the dimensions investigated, model C appears mechanically the most promising since it offers the lowest resonant frequency and induced stresses at maximum displacements. The lower resonant frequency, however, also results in reduced induced voltages in the coil for the same amplitude compared to models A and B. This is because the higher the resonant frequency results in a greater coil velocity. The simulated result of 0.38V is, however, adequate for subsequent voltage multiplication by standard step up circuits (e.g. Walton Cockcroft ladder). The discrete coils also being fabricated should increase this voltage although it does complicate the assembly process. Whilst this design will produce most power if driven constantly at its resonant frequency, it should also function from periodic excitation which will cause the paddle to oscillate thereby generating electrical energy. This mode of operation has implications for the packaging of the generator and will be the subject of future investigation.

REFERENCES

[i] E. H. Callaway, Wireless sensor networks: architectures and protocols, Auerbach Publications, chapter 7
[ii] E. P. James, M. J. Tudor, S. P. Beeby, N. R. Harris, P. Glynne-Jones, J. N. Ross, N.M. White, "An investigation of self-powered systems for condition monitoring applications", Sensors and Actuators A, 110, pp. 171-176, 2004.
[iii] P. Glynne-Jones, M. J. Tudor, S. P. Beeby, N.M. White, "An electromagnetic, vibration-powered generator for intelligent sensor systems", Sensors and Actuators A, 110, pp. 333-349, 2004.